A 50-kW Module Power Station of Directly Solar-Pumped Iodine Laser

S. H. Choi

J. H. Lee

W. E. Meador

E. J. Conway

NASA Langley Research Center, Hampton, VA 23681-0001

The conceptual design of a 50 kW directly solar-pumped iodine laser (DSPIL) module was developed for a space-based power station which transmits its coherent-beam power to users such as the moon, Martian rovers, or other satellites with large (>25 kW) electric power requirements. Integration of multiple modules would provide an amount of power that exceeds the power of a single module by combining and directing the coherent beams to the user's receiver. The model developed for the DSPIL system conservatively predicts the laser output power (50 kW) that appears much less than the laser output (93 kW) obtained from the gain volume ratio extrapolation of experimental data. The difference in laser outputs may be attributed to reflector configurations adopted in both design and experiment. Even though the photon absorption by multiple reflections in experimental cavity setup was more efficient, the maximum secondary absorption amounts to be only 24.7 percent of the primary. However, the gain volume ratio shows 86 percent more power output than theoretical estimation that is roughly 60 percent more than the contribution by the secondary absorption. Such a difference indicates that the theoretical model adopted in the study underestimates the overall performance of the DSPIL. This fact may tolerate more flexible and radical selection of design parameters than used in this design study. The design achieves an overall specific power of approximately 5 W/kg and total mass of 10 metric tons.

Introduction

Lasers permit efficient long-range transmission of electromagnetic wave energy because of their small beam divergence. Accordingly, numerous conceptual and experimental studies have been performed to explore laser systems for power transmission in space (DeYoung et al., 1988). Among them is the direct solar-pumped iodine laser (DSPIL) (Lee et al., 1988; Hwang and Tabibi, 1990). An early design study of DSPIL showed that a megawatt power output is feasible in space (DeYoung et al., 1987).

In the present study, a 50-kW DSPIL power module was considered since (a) the development of such a small unit is technologically and economically feasible, (b) the combination of several modules, as shown in Fig. 1, can be adopted for higher power demand, and (c) each module could be designed to provide power according to a user's need. The power level of the module is suitable for powering a lunar or Martian surface rover which requires a roughly 25-kW power for operation, and for powering other spacecraft. Power availability can be multiplied by directing the beams from many modules (Fig. 1).

The laser within a module is based on the master oscillator power amplifier (MOPA) principle and is composed of a master oscillator (MO), a pre-amplifier (PreAmp), a power amplifier (PA) (Fig. 2). An output of 10 W from the MO is amplified to 4 kW at the PreAmp, then this 4-kW laser beam is amplified to 50 kW at the PA for transmission. The lasant chosen for this MOPA is perfluoro-*t*-butyl iodide (t-C_4F_9I) which is the most-promising lasant for solar pumping (Lee et al., 1988). The pumping wavelength for this lasant ranges of 250 nm to 350 nm with its peak at 290 nm (Fig. 3). Laser emission is at 1.315 μm.

Contributed by the Solar Energy Division of THE AMERICAN SOCIETY OF MECHANICAL ENGINEERS for publication in the ASME JOURNAL OF SOLAR ENERGY ENGINEERING. Manuscript received by the ASME Solar Energy Division, Dec. 1993; final revision, Mar. 1997. Associate Technical Editor: R. A. Crane.

The results of our 50-kW module study were the conceptual design, the sizes, and masses of subsystems, and an energy budget, including thermal, mechanical, electrical, and laser energy. A key element of the conceptual design of the module is that lasant and coolant pipes also provide much of the structure of the system.

General Layout of the Module

This laser power module consists of a three-stage iodine MOPA with solar concentrators, a set of resonator mirrors, beam-steering optics, a lasant circulation loop with a pump, and a radiator. The overall configuration is shown in Fig. 2. Other elements include lasant storage tanks (LST) and a control moment gyroscope (CMG). The LST are designed to hold sufficient amount of lasant for sustaining the operation over five years. The CMG is used to keep the power station oriented with the solar concentrator axis pointed directly at the sun.

The main solar concentrator has a hexagonal frame for easy integration with other modules (see Fig. 1). The area between the aperture of concentrator and hexagonal frame is covered by a photovoltaic cell panel that provides the power required for DSPIL module operation. The solar concentrator focuses solar flux into the power amplifier (PA). The iodine master oscillator (MO) and preamplifier (PreAmp) use their own solar concentrators for laser pumping.

The amplifier is composed of a double-layered quartz tube (Fig. 4). The annular space between tubes is used for active cooling of the quartz laser cavity. The lasant material that passes through the PA is also heated and thus requires heat dissipation to maintain the lasant temperature below 500 K for laser kinetics of the returning lasant. The MO and PreAmp are designed to use a low solar concentration, so that they do not require any active cooling of laser cavity. The PA tube has 12 branches of circulation outlets and inlets, respectively. The six circulation loops are for lasant cooling and the other six loops for cooling the quartz tubes. The pipes, which comprise both lasant and coolant loops, also provide mechanical supports to the MOPA

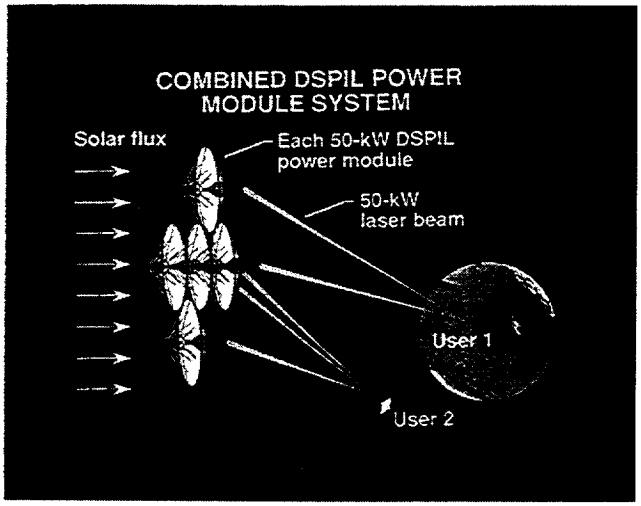

Fig. 1 An artistic rendition of a laser power satellite that integrates several 50-kW DSPIL power modules

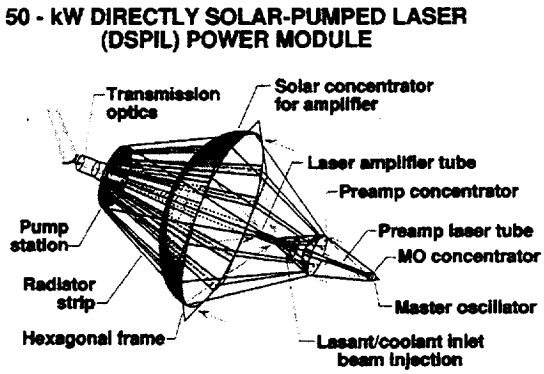

Fig. 2 Configuration of a 50-kW DSPIL power module

system. Each loop has its own pump and flow controller. Thus, if one of the six circulation loops malfunctions, the functioning loops take over and still maintain a proper circulation of the lasant or coolant. The flow rates of lasant and coolant are generally determined by the amounts of thermal loading to the laser tube and lasant, respectively.

The MO produces continuous wave (CW) power. This CW laser beam could be modulated at a frequency of 1 kHz by an acousto-optics modulator. Whether CW or pulsed, the beam is expanded, collimated, and injected into the PreAmp for initial power amplification. Since a small low-power laser cavity with a spatial filter produces a single transverse mode to yield Gaussian beam profile, the master oscillator is designed as a small low-power system. If a high quality beam from the PreAmp is injected into the PA, then the amplifier can produce a high quality beam suitable for long distance transmission. The beam amplified by PA enters the beam-steering optics (BSO) where the beam is expanded to the size of the steering reflector and aimed toward a user. The PA equation was derived for the estimations of power requirements of PreAmp and PA:

$$P = P_o + W_p N_L V h\nu - P_s \ln\left(\frac{P}{P_o}\right) \quad (1)$$

where P is the amplified power output from PreAmp or PA, P_o

Nomenclature

A = Einstein coefficient of emission transition probability
A_{34} = Einstein coefficient (5.1 for t–C_4F_9I) defined at a specific quantum level transition probability
A_c = aperture area of solar concentrator
A_q = side wall area of a frustum-like focal volume
A_{ref} = reflective surface area of concentrator
A_s = area of laser cavity side wall
A_t = cross section area of laser cavity
c_p = specific heat of medium
c_{pw} = specific heat of water
C_g = geometric correction constant
C_q = absorption constant of solar energy through quartz tube wall
C_m = absorption constant solar energy by medium
d = one absorption length for $N_L\sigma d = 1$
D = diameter of laser cavity
D_H = hydraulic diameter of a circular tube annulus
D_p = path distance of photon in the medium
f = focal length of parabolic solar concentrator
$F(\lambda)$ = solar spectral photon fluence
F_{ex} = view factor between laser cavity and concentrator
g_o = unsaturated energy gain = $W_p N_L \sigma_s \tau$
h = Planck's constant
I = atomic iodine
I* = excited atomic iodine
k_2 = rate coefficient for $R + I \rightarrow RI$
K = attenuation coefficient of solar flux in water
L = length of laser cavity
M = geometric magnification parameter
N_B = number density of buffer gas (argon)
N_L = molecular number density of lasant (t–C_4F_9I)
p_B = pressure of buffer gas
p_L = pressure of lasant
P = amplified power output
P_i = unsaturated power = $W_p N_L V \sigma_s \tau$
P_o = injected laser beam power into PreAmp or power amplifier
P_s = saturated power = $h\nu A_t / \sigma\tau$
P_S = solar power required for DSPIL system
P_w = solar power absorbed by cooling water
Q_1 = rate coefficient for lasant (t–C_4F_9I
Q_2 = rate coefficient for buffer gas (argon)
r = reflectance of oscillator output mirror
r_q = radius of laser cavity
R = radicals of perfluoalkyl-iodides
Re = Reynolds number
S = solar constant = 1.353 kW/m^2 at air-mass zero
S_c = solar concentration rate
S_{cv} = thermal power removal by convection
S_{ec} = radiative exchange with the solar concentrator
S_{es} = radiative loss from laser cavity to space
S_m = power remaining in the lasant medium after lasing
S_q = solar flux absorbed by quartz tube
S_{ref} = solar flux reflected from concentrator surface
S_w = solar flux absorbed by cooling water
T_c = solar concentrator temperature
T_q = quartz tube temperature
ΔT = laser medium temperature between inlet and outlet of laser cavity
ΔT_w = water temperature difference between inlet and outlet
V = active volume of laser cavity
v_m = medium flow velocity in the laser cavity
v_w = cooling water flow velocity through annular space of laser cavity
W_p = pumping rate per molecule

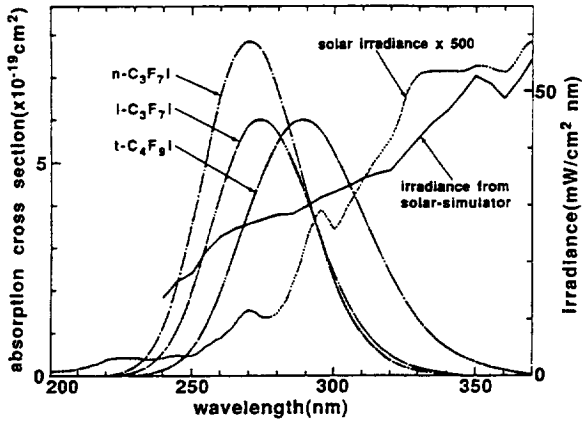

Fig. 3 The absorption cross sections of iodine and the AM0 solar irradiance compared with the measured irradiance from the solar simulator

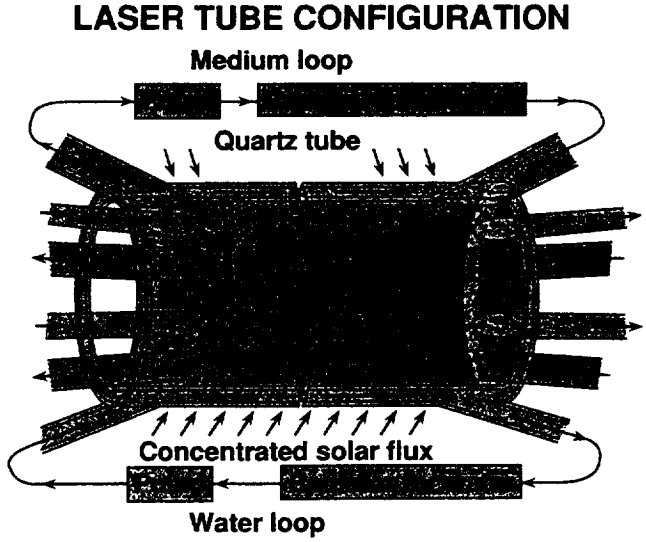

Fig. 4 Configuration of the DSPIL laser tube

the input power to PreAmp or PA, W_p the pumping rate, N_L the molecular number density of lasant, V the active volume, h the Planck's constant, ν the frequency of light wave, and P_s the saturation power which is described by

$$P_s = \frac{h\nu A_t}{\sigma_s \tau} \tag{2}$$

where A_t is the cross-sectional area of a laser tube, σ_s the cross section of stimulated emission, and τ the life time of an excited iodine atom and determined by

$$\frac{1}{\tau} = A + Q_1 N_L + Q_2 N_B \tag{3}$$

where A is the Einstein coefficient, Q_1 and Q_2 are the rate coefficients defined, respectively, for t-C_4F_9I molecules and buffer gas, and N_B the molecular number density of buffer gas argon. The cross section of stimulated emission (σ_s) is largely dependent on the partial pressure of the lasant (t-C_4F_9I) (Brederlow et al., 1983, p10) and determined by

$$\sigma_s = \frac{7 A_{34} \lambda^2}{48\pi^2 \Delta\nu} \tag{4}$$

where A_{34} is the Einstein coefficient (5.1 for t-C_4F_9I) defined at a specific quantum level (in this case, 3 to 4) transition probability, and λ the lasing wavelength (1.315×10^{-6} meter). The collisional frequency of pressure-broadened iodine laser spectrum is derived as a pressure dependent:

$$\Delta\nu = 0.15 \cdot p_L \cdot 1.333 \times 10^8 \text{ Hz}. \tag{5}$$

The pumping rate per molecule, W_P (# of photons absorbed/sec/molecule), is determined by (Lee and Conway, 1991)

$$W_P = \frac{A_s}{N_L V} \int_0^\infty F(\lambda)\eta(\lambda)\,[1 - e^{-\sigma_a(\lambda) N_L D_p}]\,d\lambda \tag{6}$$

where $A_s(\text{cm}^2)$ is the area of side wall, $N_L(\text{cm}^{-3})$ the lasant number density, V (cm^3) the volume of the laser tube, $F(\lambda)$ the solar spectral photon fluence, $\eta(\lambda)(\simeq 1)$ the spectral quantum yield, $\sigma_a(\lambda)(\text{cm}^2)$ the absorption cross section of lasant molecules, and $D_p(\text{cm})$ the path length of a photon in the medium.

Components Design

Power Requirements. The power level required for lunar and Martian surface rovers is in the range from 15 kW to 25 kW (Petri et al., 1990). Considering the conversion efficiency (43 percent, from beam power to electrical power) (Walker and Heinbockel, 1988), the power output of the module to be considered in the design has to be at least 50 kW.

The design parameters for the PA to produce 50 kW are selected or determined as follows: the average temperature of

Nomenclature (cont.)

α = angle subtended by the sun's diameter = 9.305×10^{-3} radian
γ = density of medium
ϵ_c = total emissivity of concentrator
ϵ_n = total emissivity of quartz
η_a = absorption efficiency of solar spectrum through medium
η_e = extraction efficiency of laser cavity = $1 - \ln(P/P_o)/g_o L$
η_g = effectiveness due to geometrical form factor of laser cavity
η_L = Laser quantum efficiency
η_{r1} = reflectance of solar flux at concentrator surface
η_{r2} = reflectance of solar flux at quartz tube surface
η_s = absorption percentage of solar spectrum by lasant
$\eta_{t1\&t2}$ = transmittances of inner and outer quartz tubes
η_{t3} = transmittance between water and quartz wall
θ = angle between impinging and reflected solar fluxes on concentrator
θ_o = angle between the optical axis and the rim of center hole of concentrator
$\theta_{\max}$ = angle between the optical axis and the aperture rim of concentrator
κ = thermal conductivity
λ = wavelength of iodine laser = 1.3152 μm
μ = viscosity
ν = frequency of light wave
$\Delta\nu$ = collisional frequency of pressure-broadened iodine laser spectrum
σ = Stefan-Boltzmann constant
$\sigma_a(\lambda)$ = absorption cross section of lasant molecule
σ_s = cross section of stimulated emission
τ = upper level lifetime of excited lasant molecules

lasant in the laser tube, $T_{[RI]}$ = 380 K, the lasant pressure, p_L (t-C_4F_9I) = 3.6 torr, the molecular number density, N_L (at 380 K) = 1.15×10^{23} m^{-3}, the buffer gas pressure, p_B (argon) = 760 torr, the molecular number density, $N_B = 2.43 \times 10^{25}$ m^{-3}, the diameter of laser tube, D = 0.3 m, the tube length, L = 5 m, the cross-sectional area of tube, $A_t = 7.07 \times 10^{-2}$ m^2, the upper level life time, $\tau \simeq 1.07 \times 10^{-2}$ sec, and the pumping rate with 1180 times AM0 solar concentration, $W_p = (7.69 \times 10^{-3})(1{,}180) = 9.08$ sec^{-1} (see Table 1). In Eq. (1), the second term becomes 55.9 kW and P_s = 3.66 kW when $\sigma_s = 2.73 \times 10^{-22}$ m^2 which is estimated by the pressure-broadening assumption. Using these parameters for Eq. (1) the laser power output (P_o) required for the PreAmp is obtained. The PreAmp power must provide 4-kW laser power to the PA.

The parameters of the 4-kW PreAmp are selected or determined as $p_L(t$-$C_4F_9I)$ = 10 torr, N_L(325 K) = 3.24×10^{23} m^{-3}, p_B(argon) = 760 torr, $N_B = 2.43 \times 10^{25}$ m^{-3}, D = 0.1 m, L = 1.5 m, $A_t = 78.5 \times 10^{-4}$m^2, $\tau = 4.26 \times 10^{-3}$ sec, $W_p = (8.17 \times 10^{-3})$ (160) = 1.307 sec^{-1}, $\sigma_s = 2.5 \times 10^{-22}$ m^2, and $g_o = W_pN_L\sigma_s\tau = 4.51 \times 10^{-3}$. The second term of Eq. (1), $P_i = W_pN_LVh\nu$, becomes 7.54 kW. The input power, P_o, from MO is selected as 10 W, then the extraction efficiency, $\eta_e = \ln (P/P_o)/g_oL = 0.98$. With these parameters, the 4 kW of power output from PreAmp by Eq. (1) is obtained.

The power output from the MO was derived as follows:

$$P = P_i\left[1 - \frac{5 \ln M}{6g_oL}\left\{1 + 0.2\left[1 + \frac{6W_pN_L}{k_2}\left(\frac{\sigma_sL}{\ln M}\right)^2\right]^{1/2}\right\}\right] \quad (7)$$

where $\ln M = 0.5 \ln (1/r)$, the mirror reflectance r = 0.85, L = 1 m, D = 0.03 m, $\sigma_s = 3.3 \times 10^{-22}$ m^2, $g_o = 1.91 \times 10^{-3}$, $k_2 = 0.6 \times 10^{-17}$ m^3/molecules · s (Brederlow et al., 1983, p. 44; Krug and Witte, 1982), $N_L = 5.084 \times 10^{23}$ m^{-3}, $\tau = 2.75 \times 10^{-3}$ sec, $W_p = 0.828 \times 10^{-2}$ sec^{-1}, and P_i = 22.5 W. Using these parameters for MO, the 11 W of power output is obtained.

System Efficiencies. The laser tube is designed to accommodate the solar image into it. Thus, the thermal load to the medium is quite high. To dissipate such a high thermal load, a double-layered quartz tube was adopted (Fig. 4). Pure water is used as the coolant because the absorption band of water lies at a shorter wavelength than the pumping band of the lasant. For reasonable values of the water attenuation coefficient (Driscoll and Vaughan, 1978) at the pump-band wavelength and for a 0.025-m thickness of the water jacket, the transmittance (η_w) is greater than 99 percent. Thus, the water pocket attenuates the pumping power by only an insignificant amount. The same cooling method was used in the laboratory-scale DSPIL experiments, and there was no measurable amount of attenuation observed.

Table 1 Path lengths and pumping rates

D_p cm	$p_L \cdot D_p$ (torr · cm)	W_P [$\times 10^{-2}$] sec^{-1} per 1 sc
72.9	262.4	0.8292
72.8	262.1	0.8289
72.7	261.7	0.8282
72.4	260.6	0.8270
72.0	259.2	0.8252
71.5	257.4	0.8230
70.9	255.2	0.8202
70.2	252.7	0.8167
69.3	249.5	0.8126
68.3	245.9	0.8077
67.1	241.6	0.8019
65.8	236.9	0.7952
64.3	231.5	0.7872
62.6	225.4	0.7778
60.7	218.5	0.7664
58.7	211.3	0.7573
56.6	203.8	0.7458
54.0	194.4	0.7372
51.3	184.7	0.7282
48.0	172.8	0.7170
44.4	159.8	0.7053
40.5	145.8	0.6944
36.4	131.0	0.6789
31.9	114.8	0.6685
27.0	97.2	0.6553

*: The average path length is 59.3 cm.

*: The average pumping rate is 0.7694×10^{-2}.

A 90 percent reflectance (η_{r1}) is used for the concentrator at the pumping wavelength. The reflection of solar flux at a vacuum-quartz surface is five percent. Thus, the rest (η_{r2} = .95) enters quartz tube. The transmittance (η_{t1} & η_{t2}) of quartz tubes is 0.98. The transmittance (η_{t3}) between water and quartz is unity since the refractive indices of water and quartz are almost the same. The laser quantum efficiency (η_L = 0.2205) is defined as the ratio of the photon energy ($h\nu$) at the stimulated emission wavelength (1315 nm) to the average photon energy at the absorption band (250 ~ 350 nm). This efficiency signifies that a portion of solar spectrum absorbed along the ray path length (η_a) by the medium is converted into laser output. The absorption band of t-C_4F_9I ranges from 250 nm to 350 nm as shown in Fig. 3. The solar spectral irradiance within this bandwidth is approximately four percent (η_s). This portion of the solar spectrum passes through the lasant medium and is partially absorbed during passage. The lasant, t-C_4F_9I, is transparent to the rest of the solar spectrum.

The absorption length, d, is defined as $d = 1/[N_L\sigma_a]$, where σ_a is the optical absorption cross section per molecular and N_L the molecular number density. The effective absorption cross section, σ_a, of t-C_4F_9I is roughly estimated as 2.0×10^{-23} m^2 using the maximum absorption cross section from Krug and Witte (p. 3, 1982). The partial pressure of the t-C_4F_9I is 3.6 torr over an average path length (D_p) of 0.593 m. The number density at this pressure is 1.18×10^{23} m^{-3}. Hence, the absorption length, d, equals 0.424 m. Therefore, the absorption, $\eta_a = 1 - e^{-(D_p/d)}$, along the path becomes 0.753. The geometrical form factor, η_g(0.8488), is determined for the geometrical arrangement between concentrator and laser tube (see Appendix). The extraction efficiency, η_e, becomes nearly 100 percent for long pulse extraction (Hwang and Han, 1984).

The total system efficiency is

$$\eta_{sys} = \eta_L\eta_s\eta_a\eta_{t1}\eta_{t2}\eta_{t3}\eta_{r1}\eta_{r2}\eta_w\eta_g\eta_e = 4.594 \times 10^{-3}. \quad (8)$$

Therefore, the solar energy required for a 50-kW module system is $P_S = P/\eta_{sys}$ = 10,884 kW. The solar concentration within the focal volume formed inside the laser cavity is represented by $S_c = \eta_{t1}\eta_{t2}\eta_{t3}\eta_{r1}\eta_{r2}\eta_w\eta_gP_S/(S \cdot A_s)$ which is equivalent to 1178 times AM0 solar constant (S) per focal volume of laser cavity (0.3 m in diameter and 5 m long).

Solar Concentrator. The concentrator for the 50-kW module requires an aperture area, A_c, of 8044 m^2. The concentrator is a parabolic dish with a central hole which is framed by the six branched-circulation outlets from the PA. The diameter of the central hole is 14.3 m. The six branched-circulation outlet tubes are extended to the pump station which also supports a transmission mirror (Fig. 2). The aperture diameter of the concentrator is 102 m.

The concentrator is a pseudo-parabolic dish which is increasingly opened outward from a true parabolic surface. The focal length of the true parabolic concentrator is 33.6 m. The surface area of the concentrator (approximated by a parabolic dish) is 13,687 m^2. The hexagonal frame has 118-m diagonals, and the rim area of hexagon after subtracting the aperture area is 1,000 m^2. The total area of the concentrator is the area of concentrator

plus the rim area of hexagon, which is 14,687 m^2. The rim area is used for solar photovoltaic cells which will provide 250 kW electric power for system operation.

The weight of the concentrator without supporting frames is estimated as approximately 1469 kg by using the mass density of 0.1 kg/m^2 (Canady and Allen, 1982). The frame structure is formed by a set of radiator and circulation loops. This structure serves not only as circulation loops, but also as a strong frame for concentrator. The weight of circulation loops will be discussed below.

Laser Tube. In this design, 5 m and 0.30-m are chosen for the length and diameter of the laser tube, respectively. The path length of each ray through the laser medium in the tube varies with its orientation within the angle subtended by the sun's diameter, α, and with the angle of reflection, θ. The size of the image of solar disk on a focal plane varies along the length of laser tube as a function of the angle θ given in the Appendix. The pseudo-parabolic concentrator forms a frustum-like focal volume. Hence, the size of laser tube is matched to the frustum-like focal volume. The intensity of impinging ray onto the focal plane may also vary with ray's propagation depth through the lasant medium. It also varies with density profile of the lasant (t-C_4F_9I) molecules in the cavity if the density profile is not uniform. The path length D_p can be geometrically approximated by assuming that it is the same as the tube diameter. However, taking the oblique angle of the impinging rays into account, an average ray travels a longer distance than the tube diameter.

The pumping rates were computed by considering the geometrical and spectral aspects and the density profile together. Table 1 shows the pumping rates with respect to the path lengths. The rays impinge to the laser cavity with angles from 12 deg to 75 deg. Thus, the path lengths are greater than the diameter of laser cavity. Figure 5 shows the profile of pumping rate along the radial direction. The absorption through lasant is exponentially decayed across the cavity. However, the rays impinge on the cavity by all directions. The pair of rays that are opposite each other is superposed along the path. The result of superposed pair is given in Fig. 5. The results also contribute the formation of Gaussian profile of laser output beam.

Thermal Loads. The thermal load on the outer quartz tube of laser cavity by impinging solar flux is estimated by the equation given in the Appendix,

$$S_{q1} = C_g C_q \frac{S_c f}{\alpha L} \simeq 15{,}768 \quad \text{W/m}^2 \tag{9}$$

where $C_g = 1.082$, $C_q = \eta_{r1}\eta_{r2}(1 - \eta_{t1})$, $S = 1.353$ kW/m^2, f the focal length (33.6 m), α the angle subtended by the sun's

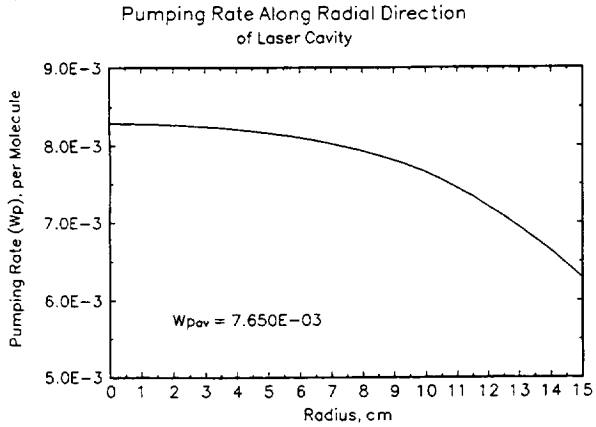

Fig. 5 Pumping rate distribution of t-C_4F_9I lasant molecule across the laser cavity

Table 2 Lasant medium parameters

Parameter	t-C_4F_9I	Argon	Mixture*
c_p (J/kgK)	621.4	521.58	526.09
γ (kg/m^3)	0.0073	1.784	1.776
M $(g/mole)$	346	39.948	53.79
μ,[$\times 10^{-8}$] $(kg/m \cdot sec)$	1310	2006	1975
κ,[$\times 10^{-5}$] $(J/m \cdot sec \cdot K)$	719	1720	1675

† from Krug and Witte (1982).
* for 3.6 torr t-C_4F_9I and 760 torr argon.

diameter (9.3048×10^{-3} radian), and L the length of laser tube. For the inner quartz tube, $C_q = \eta_{r1}\eta_{r2}\eta_{t1}\eta_w(1 - \eta_{t2})$ and $S_{q2} = 15{,}298$ W/m^2. The absorbed energy, $S_q = S_{q1} + S_{q2}$, dissipates through radiation and convection. Thus

$$\begin{aligned} S_q &= S_{es} + S_{ec} + S_{cv} \\ &= (1 - F_{ex})\epsilon_n \sigma T_q^4 + F_{ex}\sigma(\epsilon_n T_q^4 - \epsilon_c T_c^4) + S_{cv} \end{aligned} \tag{10}$$

where S_{es} is the radiative loss to space, S_{ec} the radiative exchange with concentrator, S_{cv} the convective heat removal, F_{ex} the view factor which is approximately 40 percent due to the geometrical formation selected in this design, ϵ_n the total emissivity of quartz (=0.932), T_q the quartz tube temperature, and T_c the concentrator temperature. Without considering the heat removal by convection (S_{cv}), the radiatively cooled quartz temperature would be 877 K. When 92 percent of the heat is removed from the quartz by the coolant, the quartz temperature is reduced to 471 K.

The power to be dissipated by the lasant medium (per unit wall area) after lasing may be estimated using Eq. (9) with a slight modification.

$$S_m \simeq C_g C_m \frac{S_c f}{\alpha L} \simeq 17{,}602 \quad \text{W/m}^2 \tag{11}$$

The coefficient, $C_m = \eta_{r1}\eta_{r2}\eta_{t1}\eta_{t2}\eta_{t3}\eta_a\eta_w\eta_s(1 - \eta_L)$, determines the fraction of the absorbed power density to be removed from the medium after lasing. In term of power, $P_m = S_m A_s = 83$ kW. For stable operations, this amount of power has to be removed also from radiator to return the laser medium to its appropriate inlet temperature. The designed inlet and outlet temperatures of medium in the laser tube are 280 K and 480 K, respectively. Flow of the lasant medium carries away some of the absorbed energy from the active volume. The medium velocity in the tube may be expressed by

$$V_m = \frac{S_m A_s}{\gamma A_t c_p \Delta T} \tag{12}$$

where A_s is the area of the tube side-wall, γ is the density of the fluid in kg/m^3, A_t is the cross-sectional area of the tube, and c_p is the specific heat of the fluid. Table 2 lists the parameters of the lasant and buffer gases. For $A_s = 4.7124$ m^2, $A_t = 0.0707$ m^2, $\gamma = 1.776$ kg/m^3, $c_p = 526.09$ J/kgK, and the 200 K temperature difference allowed between the inlet and outlet of the laser cavity to maintain the medium temperature at the exit below the pyrolytic point (500 K) of the lasant, the medium velocity is 6.28 m/sec.

In this design, the medium velocity is increased to 10 m/sec to keep the medium temperature well below the pyrolytic temperature of t-C_4F_9I. With this velocity, the temperature difference between the inlet and outlet of laser tube becomes 137 K.

The distilled water has a broad absorption band beyond 0.4 μm of solar spectrum (Driscoll and Vaughan, 1978, p. 15–28 and p. 15–29) and the absorption by water accounts for

approximately 5.88 percent of impinging solar power. For a 5-cm thick water in an annular channel and 1180 AM0 solar constants, the total absorbed solar flux by water (S_w) is 62,173 W/m^2. This coolant water needs to remove the solar fluxes absorbed by both the quartz tubes and cooling water ($S_q + S_w$ = 93,239 W/m^2). The design sets the maximum outlet temperature of water in the laser cavity to be 350 K by allowing 70 K raise from 280 K inlet temperature of water. To keep the water under boiling point, the maximum 17 K difference between quartz walls and water at the outlet of a laser cavity is allowed. These design tolerances require 1.75 m/sec (Re = 10^5) flow velocity of cooling water (Pr = 4.86) in the annular channel (D_H = 0.1 m). The heat transfer rates estimated for the annular channel (Kays, 1966) to remove this amount of heat flux (S_{q1} and S_{q2}) are 3154 W/m^2·K and 3382 W/m^2·K, respectively, for the outer and inner quartz tubes. The temperature differences are 14.7 K and 13.9 K which are within the design tolerances. The water flow velocity determined above is adequate for operation, but increased to 2.0 m/sec for safety.

The heat removal system includes the coolant pumping station, the lasant circulation loop with radiators, and the water loop with radiators. This system removes heat from the lasant medium and quartz tubes. The estimated weight of this system is 4212 kgs.

Lasant Medium. The formation of I_2 molecules has a quenching effect on excited iodine atoms I^*. The high quenching rate of I^* reduces laser power output and efficiency. The quenching rate coefficient, Q_1, for t-C_4F_9I molecules is not well defined yet. The rate coefficients used in the calculation may be found from Brederlow et al. (1983). Since t-C_4F_9I molecules exhibit little or no irreversible radical dimerization (Zalesskii, 1983), t-C_4F_9I molecules circulating with the 10 m/sec velocity in the DSPIL cavity leave no steady-state concentration of I_2, except a low initial concentration of iodine molecules. The dwell time of medium in the cavity is slightly less than a second.

The quenching effect of the excited iodine molecules by argon at one atmospheric partial pressure is negligible as compared to the quenching effects by other molecules. For instance, using the parameters illustrated on Tables 2.5 and 2.6 of Brederlow et al. (pp. 44–45, 1983), argon, at 760 torr pressure, allows approximately five kinetic reactions ($I^* + Ar \rightarrow I + Ar$) within the dwell time. With t-C_4F_9I (RI) at 3.6 torr, 90 kinetic reactions ($I^* + RI \rightarrow I + RI$) take place within the cavity. On the other hand, the atomic iodine (I) after laser action recombines with radical (R). This regenerative kinetic process ($R + I \rightarrow RI$) is the most favorable and dominant feature of the lasant t-C_4F_9I. Within the dwell time, 7.64×10^5 regenerative kinetics are expected.

At low temperature, the pyrolytic production of I_2 is negligible. Zalesskii (1983) reported that at below 400 K no trace of I_2 appeared. And a recent laboratory test (Miner, 1991) shows no trace at 523 K, indicating a higher pyrolytic temperature. In the design, the medium temperature becomes 443 K in the safe range from pyrolytic. Since this lasant temperature is at an outlet, the active region of medium remains below this temperature.

The lasant consumption due to chemical kinetics and pyrolytic for any service life of the laser is not a significant issue as reported by Zalesskii (1986). In space, the leakage control could be a major issue.

Master Oscillator (MO). The minimum output power required from MO for the preamplifier is 10 W. The solar energy required for pumping at 10-W MO power is 6.34 kW. The low solar concentration (S_c = 50 times AM0) on the MO laser tube (0.05 m dia. and 1 m long) does not require any active cooling system. From Eq. (10) without convective cooling, the temperature of laser tube is obtained as 434 K. However, the circulation of lasant in the tube is required to avoid I_2 formation by pyrolytic. The velocity has to be 0.041 m/sec. The rest of the parameters are illustrated in the first column of Table 3.

Pre-amplifier. The laser tube is stretched to 15 m to achieve both a reduction of solar concentration and exponential gain saturation. Since low solar concentration (S_c = 160 times AM0) onto the PreAmp tube is employed, no active cooling of the laser tube is necessary. From Eq. (10), the temperature of the laser tube is 353 K. The thermal load to medium is 46 kW. Thus, the flow velocity to remove 46 kW becomes 2.2 m/sec when constrained by a 200 K temperature increase for medium. The rest of parameters are listed in the second column of Table 3.

Results of Laboratory Work

The laboratory-scale DSPIL experiments have been the main thrust of the effort to prove and validate the concept and to find better lasant materials (Lee, 1984). The experimental setup consists of a solar simulator (40-kW optical power output), an elliptical reflector enclosure, a lasant circulation loop, and a laser cavity. The laser cavity for experiments has the same annular quartz tube of which annular space is used for coolant passage. The results are chronologically tabulated in Table 4.

Experiments could have been the basis for establishing the design of the DSPIL system. A scaling-up estimation of laser power based on experimental results is possible. The laser output is proportional to the active volume of the laser cavity and the input solar intensity (S). Extrapolation of the experimental data to the active volume (V) of the 50-kW DSPIL system gives approximately 110-kW output. Considering the form factor correction (η_g = 0.8488) because of the frustum-like formation of focal volume, the laser output power becomes 93 kW. This is approximately 1.8 times more than the design value, 50 kW. Thus, the 50-kW DSPIL system may be able to generate more power than designed. On the other hand, for a 50-kW operation the loads (thermal, mass, optical power) can be relaxed and the overall weight estimated in this design study can be drastically reduced. Even though the theoretical modeling significantly underestimates the laser output power, the difference does not indicate a problem with the theoretical model. This difference may also be attributed to the difference in configurations that were used in the design and experiments (i.e., a parabolic reflector versus an elliptic reflector).

Concluding Remarks

A method of design for a 50-kW direct solar pumped iodine laser was conceptualized. Concentration of solar energy to a size of laser tube is essential for maximizing the use of solar energy. Therefore, modification of a true parabolic dish reflector to the pseudo-parabolic dish enables a formation of a frustum-

Table 3 Parameters for MO, PreAmp, and PA

Parameter	MO	PrA	PA
Output Power	0.01 kW	4	50
η_{sys}, [$\times 10^{-3}$]	3.26	5.14	4.05
Solar Power	5.07 kW	778	12,361
Aperture Dia.	2.5 m	32	111
A_{ref}	5.65 m^2	896	11,887
Laser Tube Dia.	0.05 m	0.1	0.3
Solar Concentration, S_c	40	235	1,180
Tube Length	1 m	15	5
Lasant, torr	20	10	3.6
Buffer, torr		76	76
W_P, [$\times 10^{-2}$]	0.79	0.79	0.68
Path Length	7.46 cm	14.92	44
Medium Velocity	0.05 m/s	3.15	6
Radiator Power	- kW	46	296
Radiator Area	- m^2	70	368
Weight	50 kg	1,600	9,075

Table 4 Performances of laboratory-scale DSPIL

Year	Iodide	V cm^3	S sc	P Watt	Ref.
1981	n-C_3F_7I	16	~10,000	4	Lee and Weaver (1981)
1986	n-C_3F_7I	30	~ 1,300	10	Lee, Lee, and Weaver (1986)
1989	t-C_4F_9I	47	~ 1,000	14	Lee et al. (1989)
1990	n-C_3F_7I	153	~ 1,000	20	From laboratory notes (1990)
1992	i-C_3F_7I	203	~ 1,300	30	Tabibi et al. (1992)
1993	t-C_4F_9I	203	~ 1,000	46	Tabibi et al. (1993)

like focal volume. The thermal loads have been estimated for design of components. The design provides some details of the DSPIL system and defines many system requirements.

The 50-kW DSPIL system is a simple and easily achievable concept. Currently, technology and knowledge base required for most of the system components are available. The laboratory efforts were confined to the use of an available source, 40-kW optical power for a laboratory-scale DSPIL experiment. Further development of a theoretical model for the DSPIL is necessary and eventually provide a scaling law so that experimental results can be interpreted for a full-scale DSPIL system.

The weight estimation in Table 3 is made for the five-year operational system. The weight could be reduced by intelligent selection of materials and tight design. The overall design weight of a 50-kW DSPIL is 10,725 kg and the specific power of 4.7 W/kg.

References

Brederlow, G., Fill, E., and Witte, K. J., 1983, *The High-Power Iodine Laser*, Springer-Verlag, Berlin.

Canady, Jr., J. E., and Allen, Jr., J. L., 1982, "Illumination From Space With Orbiting Solar-Reflector Spacecraft," NASA TP-2065.

Choi, S. H., 1991, "Pumping Rates based on Geometrical Aspect," NASA TM-104091.

De Young, R. J., Walker, G. H., Williams, M. D., Schuster, G. L., and Conway, E. J. 1987, "Preliminary Design and Cost of a 1-Megawatt Solar-Pumped Iodide Laser Space-to-Space Transmission Station," NASA TM-4002.

De Young, R. J., Lee, J. H., Williams, M. D., Schuster, G., and Conway, E. J., 1988, "Comparison of Electrically Driven Lasers for Space Power Transmission," NASA TM-4045.

Driscoll, W. G., and Vaughan, W., 1978, *Handbook of Optics*, Section 15 (by John E. Tyler), McGraw-Hill, New York, p. 15-1.

Hwang, I. H., and Han, K. S., 1984, "A Solar Pumped Iodine Laser Amplifier," *LIA Symposia Proceedings*, Vol. 47, ICALEO'84, pp. 87–91.

Hwang, I. H., and Tabibi, B. M., 1990, "A Model for a Continuous-Wave Iodine Laser," *Journal of Applied Physics*, Vol. 68, No. 10, p. 4983.

Kays, W. M., 1966, *Convective Heat and Mass Transfer*, McGraw-Hill, New York, pp. 176–177.

Krug, J. K. G., and Witte, K. J., 1982, "Physical and Chemical Data of Substances Related to the Atomic Iodine Laser," Max-Planck-Institut Für Quantenoptik, Report No. MPQ-61, p. 4.

Lee, Ja H., and Conway, E. J., 1991, "Power Laser Beaming and Applications in Space," *Journal De Physique IV*, Colloque C7, supplèment au Journal de Physique III, Vol. 1, pp. C7–715.

Lee, Ja H., and Weaver, W. R., 1981, *Applied Physics Letters*, Vol. 39, p. 37.

Lee, Ja H., 1984, "Solar-Pumped Gas Laser," U.S. Patent No. 4,424,592; June 3.

Lee, Ja H., Lee, Min H., and Weaver, Willard R., 1986, *Proceedings of the International Conference on Lasers '86*, p. 150.

Lee, J. H., Weaver, W. R., and Tabibi, B. M., 1988, "Perfluorobutyl Iodides as Gain Media for a Solar-Pumped Laser Amplifier," *Optics Communications*, Vol. 67, No. 6, p. 435.

Lee, Ja H., Tabibi, Bagher M., Humes, Donald H., Hwang, In H., and Weaver, Willard R., 1989, *CLEO'89 Conference*, Technical Digest Series, Vol. 11, paper WF22.

Miner, G. A. 1991, private communications, NASA Langley Research Center.

Petri, D. A., Cataldo, R. L., and Bozek, J. M., 1990, "Power System Requirements and Definition for Lunar and Mars Outposts," *Proceedings of the 25th IECEC*, Vol. 1, Aerospace Power Systems, p. 18.

Tabibi, Bagher M., 1990, private communication (from laboratory notes).

Tabibi, Bagher M., Heinbockel, John H., Costen, Robert C., and Lee, Ja H., 1992, *CLEO'92 Conference*, Anaheim, CA., May 10–15, paper CWG8.

Tabibi, Bagher M., Terrell, Charles A., Lee, Ja H., and Miner, Gilda, 1993, *CLEO'93 Conference*, Baltimore, MD, May 15–19, paper CWG12.

Walker, G. H., and Heinbockel, J. H., 1988, "Photovoltaic Converters For Solar-Pumped Lasers," *Proceedings of the 20th IEEE Photovoltaic Specialists Conference*, Las Vegas, NV, pp. 1013–1019.

Zalesskii, V. Yu., 1983, "Iodine Laser Pumped by Solar Radiation," *Soviet Journal of Quantum Electronics*, Vol. 13, No. 6, p. 701.

Zalesskii, V. Yu. 1986, "Gas Consumption in Pulse-Periodic and CW Operation of a Photodissociation Laser," *Soviet Journal of Quantum Electronics*, Vol. 16, No. 1, p. 21.

APPENDIX

The aperture area, A_c, of a concentrator is determined by the requirement of a solar concentration rate (1180 AM0) into a laser cavity to generate a 50-kW net laser beam power. The aperture diameter is

$$D_c = \sqrt{\frac{4}{\pi} A_c + D_i^2}$$

where D_i is the center hole diameter of a pseudo-parabolic dish. Using the maximum aperture angle, θ_{max}, which is determined by the angle between the optical axis of the concentrator and the radius, ρ', that connects the focal point to the periphery of concentrator, the maximum radius of the aperture is determined by

$$\rho'_{max} = \frac{D_o}{2 \sin \theta_{max}}.$$

The pseudo-parabolic dish that generates a frustum-like focal volume is created by opening up the aperture diameter of a true parabolic dish and subsequently deflecting a true parabolic dish backward by a few degrees of angle as shown in Fig. 6. The deflection angle will be determined according to the desired length of laser cavity. The radius of a true parabolic dish from its focal point is determined by

$$\rho = \frac{2f}{[1 - \cos(\pi - \theta)]}.$$

The radius of the deflected parabolic dish is

$$\rho' \simeq \rho + L \cos \theta',$$

where $\theta' = \theta - \beta$ and L is the length of the laser cavity. For a small deflected angle (β) and $L \ll \rho$,

$$\beta_{max} = \cos^{-1}\left[\frac{\rho^2 + \rho'^2 - L^2}{2\rho\rho'}\right].$$

The radius of a laser cavity is also determined by the forma-

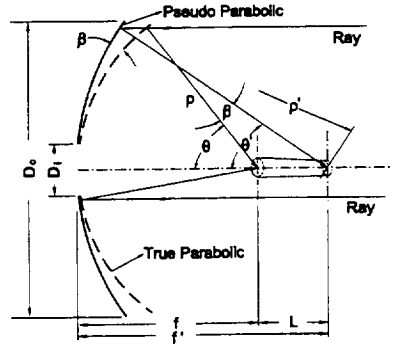

Fig. 6 A pseudo-parabolic reflector concept for a formation of frustum-like focal volume

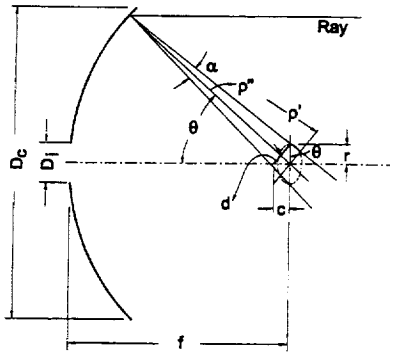

Fig. 7 A geometry for determining a geometric factor that compensates the geometrical deviation of laser cavity from the frustum-like focal volume

tion of the sun's image on a focal plane as shown in Fig. 7. The c in Fig. 7 is defined as

$$c = \frac{\rho' \alpha}{2 \cos\left(\frac{\pi}{2} - \theta\right)}$$

and

$$\rho'' = \rho' - c \sin\left(\frac{\pi}{2} - \theta\right).$$

The d in Fig. 7 is

$$d = \rho' \alpha \left[1 - \frac{\alpha}{2} \cot \theta\right].$$

The radius of the laser cavity is determined by

$$r_q = \frac{\rho' \alpha}{2} \left[1 - \frac{\alpha}{2} \cot \theta\right] \cos \theta.$$

The surface area of the concentrator, without including a hexagonal frame, is obtained by integrating the infinitesimal area over the angle from θ_o to $\theta_{\max}$.

$$A_{\text{ref}} = 2\pi \int_{\theta_o}^{\theta_{\max}} \rho'^2 d\theta.$$

The side-wall area of a frustum-like focal volume is

$$A_q = \pi(r_q + r_q')L$$

where

$$r_q = \frac{\rho \alpha}{2} \left[1 - \frac{\alpha}{2} \cot \theta\right] \cos \theta$$

and

$$r_q' = \frac{\rho' \alpha}{2} \left[1 - \frac{\alpha}{2} \cot \theta\right] \cos \theta'.$$

For $\alpha \ll 1$, $[1 - (\alpha/2) \cot \theta] \simeq 1$. Therefore,

$$A_q = \frac{\pi \alpha L}{2} [\rho \cos \theta + \rho \cos (\theta - \beta) + L \cos (\theta - \beta)^2].$$

The solar flux that reaches to the surface of a laser cavity is defined by

$$dS_q = \alpha_n \sin \theta \, dI_\theta = \alpha_n \sin \theta \frac{dS_{\text{ref}}}{A_q},$$

in which $dS_{\text{ref}} = 2\pi \eta_{r1} S \rho^2 d\theta$. Eventually,

$$dS_q = 8\alpha_n \eta_{r1} \eta_{r2} \eta_{r3} \frac{Sf}{\alpha L} \int_{\theta_o}^{\theta_{\max}} \frac{\sin \theta d\theta}{(1 + \cos \theta)\left[\cos \theta + \cos (\theta - \beta) + \frac{L}{2f}(1 + \cos \theta) \cos (\theta - \beta)^2\right]}.$$